Multiscale Computational and Experimental Analysis of Slip-GB Reactions: *in situ* High-resolution Electron Backscattered Diffraction and Concurrent Atomistic-Continuum Simulations

Yang Su[1,*], Thanh Phan[2], Liming Xiong[3], and Josh Kacher[1]

[1]School of Materials Science and Engineering, Georgia Institute of Technology, Atlanta, GA, 30332, United States
[2]Department of Aerospace Engineering, Iowa State University, Ames, IA, 50011, United States
[3]Department of Mechanical and Aerospace Engineering, North Carolina State University, Raleigh, NC, 27695, United States
* Corresponding E-mail address: ysu345@gatech.edu

Abstract: In this paper, *in situ* high-resolution electron backscattered diffraction (EBSD) is combined with concurrent atomistic-continuum (CAC) simulations to study the interactions between dislocation-mediated slip and grain boundaries (GBs) in Ni. It is found that the local stress associated with slip-GB intersections first increases upon the pileup of dislocations, then remains high even after the nucleation of dislocations in the neighboring grain, only relaxing after the nucleated dislocations propagate away from the GB due to more incoming dislocations participating in the pileup. The local stress relaxation is accompanied by an atomic-scale GB structure reconfiguration, which affects not only the subsequent dislocation transmission, but also the configuration of those dislocations away from the GB. These findings demonstrate the importance of incorporating local stress history at higher length scale models, such as crystal plasticity finite element.

Keywords: slip transfer, grain boundary, EBSD, simulation, dislocation dynamics

The mechanical properties of polycrystalline metals can be largely dictated by the interactions between dislocation-mediated slip and grain boundaries (GBs) as such interactions may generate large local stresses, promoting further slip transfer, twin nucleation, or even microcrcak formation [1,2,3]. To evaluate the likelihood of slip transfer across different GBs, various GB metrics and slip transfer models have been proposed [4,5,6,7,8]. It has been shown by extensive experimental studies that many existing metrics can be used to predict slip transfer with a good accuracy [9,10,11,12]. For instance, Nieto-Valeiras *et al.* [13] used slip trace analysis to study the slip transfer in pure Ni and concluded that slip transfer mainly occurs at GBs with m' greater than 0.8. Here, $m'=\cos\varphi\cos\kappa$, where φ and κ are the angles between slip plane normal and Burgers vectors

of the incoming and outgoing system, respectively. Despite the success of those metrics in assessing the probability of a slip transfer, few experimental studies have characterized the evolving local stress and strain fields as a function of the applied load. High resolution EBSD (HR-EBSD), a variation of traditional Hough-based EBSD that is sensitive to elastic strain gradients in crystalline materials [14,15], has been applied in a number of studies to evaluate the stress and elastic strain gradients associated with dislocation interactions [11,16]. Most recently, Koko *et al*. [16] characterized the strain fields around the tip of an incipient slip band during *in situ* scanning electron microscopy (SEM) deformation using HR-EBSD. The obtained elastic fields were then used to evaluate the stress intensity factor. Nevertheless, the evolution of a stress field ahead of a dislocation pile-up during the process of a slip transfer has not yet been experimentally quantified.

High fidelity simulations provide additional insight into the local material state associated with dislocation-GB interactions. Various modeling methods, such as molecular dynamics [17], dislocation dynamics [18], and so on [19, 20, 21], at disparate length scales have been used to study dislocation-GB interactions. For instance, Liu *et al*. [18] studied the slip transmission of dislocations with different characters through a low angle symmetric tilt GB using dislocation dynamics and found that the stress required to enable dislocation transmission through a GB varies significantly if the character of the incoming dislocation changes. Due to the multiscale nature of slip-GB interactions, involving both the atomistic structure evolution at the GB and the long-range dislocation activities away from the GB, a full-spectrum analysis of slip-GB interactions using single-scale methods remains a challenge. To address this challenge, there exists a need to leverage the strengths of many recently developed multiscale methods, such as concurrent atomistic continuum (CAC) methods [19, 22] in particular, to simultaneously retain the microscale dislocation slip as well as the atomistic GB structure evolution within one model.

In this study, the progressive evolution of the stress and strain fields ahead of dislocation pile-ups in the vicinity of several representative GBs in polycrystalline Ni was characterized *in situ* at varying strain levels using HR-EBSD. The experimentally measured local stress evolution was then compared with simulated values acquired from representative CAC simulations.

Experiments were carried out using 1 mm thick high purity (99.9995%) polycrystalline Ni purchased from Goodfellow. Dog-bone shaped tensile specimens were cut using electrical discharge machining. The specimens were annealed in an argon atmosphere at 800 ℃ for 40 min to obtain an average grain size of ~400 μm as shown in Figure 1(a). The surface was prepared for HR-EBSD analysis by grinding with silicon carbide papers (from 800 to 4000 grit) followed by diamond slurry polishing (6 μm to 1 μm) and finished with colloidal silica suspension polishing. The specimen was deformed under uniaxial tension using a Kammrath & Weiss *in situ* SEM stage at a displacement rate of 2 μm/s. The tensile test was paused (shown in Figure 1(b) as discontinuities in the stress-strain curve) at various applied strains starting from 0.12% for HR-EBSD analysis. The GBs of interest were carefully selected using secondary electron (SE) imaging to ensure that the incoming slip band had not generated any outgoing slip bands at the initially-investigated strain levels. HR-EBSD analysis was carried out in a roughly 8x8 μm area with a step size of 60 nm. All scans were conducted at 20 kV using a Velocity high speed electron detector in a TESCAN MIRA scanning electron microscope. The pattern acquisition speed was optimized by balancing between the scan time and pattern quality, as longer scan times lower the noise levels, but might induce undesired stress relaxation during the process of the formation of dislocation pile-ups.

The EBSD patterns collected in the area of interest at each applied strain level were analyzed using OpenXY (an open source software package [23]). This software package uses cross-correlation

based measurements to calculate shifts in regions of interest between each EBSD pattern in a grain and a single reference pattern. The deformation gradient tensor and the associated elastic strain and stress tensors are then derived from the pattern shifts. To quantify the stress acting on the active slip system (which is determined using slip trace analysis outlined in [8]), the resolved shear stress (RSS) was acquired by projecting the stress tensor onto the slip plane in the slip direction according to: $\mathrm{RSS} = \boldsymbol{\sigma} : (\mathbf{d} \otimes \mathbf{n})$, where $\boldsymbol{\sigma}$ is the stress tensor, $\mathbf{d}$ and $\mathbf{n}$ are unit vectors parallel to the slip direction and the slip plane normal, respectively.

The results of HR-EBSD analysis at three GBs are presented in Figures 2-4. The alignment of the incoming and outgoing slip systems for all three GBs are indicated by their m' values (m'=0.82, 0.78, 0.86 in Figure 2, 3, 4 respectively). The first row in Figures 2-4 contains image quality maps/secondary electron images showing the progression of slip transfer across GBs as the nominal applied strain increases from 0.12% to 1.16%. In all cases, the outgoing slip system(s) only initiates after the strain reaches a certain threshold. This is most obvious in Figure 3 where an outgoing slip band only becomes noticeable starting from Figure 3(a2). In Figures 2 and 4, the outgoing slip band is not as significant as in Figure 3a. This is likely due to the Burgers vector of the outgoing slip system being near- parallel to the sample surface.

The second row of Figures 2-4 shows the RSS gradient maps calculated by HR-EBSD analysis. The stress concentration induced by the incoming dislocation pile-ups can be observed in the vicinity of the slip band-GB intersections for all three cases. In addition, by comparing the pile-up induced stress at each strain level, it is found that the progression of the extent of the pile-up induced stress follows similar trends at all three GBs. More specifically, the magnitude of the pile-up stress always reaches a peak values (shown in Figure 2(b1), Figure 3(b5), and Figure 4(b1)) before declining with further increases in the applied strain (shown in Figure 2(b2), Figure 3(b6),

and Figure 4(b2)). This trend is more obvious by examining the third row of Figures 2 and 3 where the RSS values were plotted along a line parallel to the incoming slip bands and extending a few microns into the outgoing grain. It can be seen in Figure 2(c1), Figure 3(c5), and Figure 4(c1) that the pile-up induced stress reached a maximum value, after which it began to decline. In addition to the similar stress relief observed in all three cases, the maximum pile-up stress, 715MPa, 907MPa, and 395MPa, can also be obtained from the third row of Figure 2, 3, and 4.

By comparing slip transfer at those three GBs, it can be clearly seen that the dislocation pile-ups can induce significant stress concentration (as high as 400-900MPa) even at the very early stages of deformation (nominal applied strains less than 1%) or at a grain boundary with a high m' value (=0.86). It was also found that the pile-up stress (907MPa, 715MPa, and 395MPa) tends to be smaller at GBs with higher m' (0.78, 0.82, and 0.86). This negative correlation is likely caused by the larger barrier strength of GBs with lower m' values, leading to higher local stress values needed for dislocation transmission. The decrease in pile-up stress observed after reaching a peak magnitude in all three cases is thought to be caused by the emission of dislocations into the neighboring grain. The variations in the local stress state may also be related to the interaction of absorbed dislocations with the pre-existing intrinsic grain boundary dislocation content [24], though the experimental and computational tools used in this study are not able to resolve such interactions.

To shed further light into the atomic-scale processes accompanying the dislocation-GB interactions, a CAC model was built with experimental inputs (grain orientations and GB plane orientation) to simulate the slip transfer studied in Figure 2 ($m' = 0.82$). As a brief review, CAC modelling is a finite element implementation of an atomistic formulation that has been introduced in previous work [19, 21, 25, 26]. It combines the atomistic description of the GBs and the coarse-

grained atomistic description of materials away from the GB within one model. In this study, a bi-crystal model was built, with the two grains separated by a twist GB with a disorientation angle of $\theta = 34.48°$ about the $[\overline{1}\overline{1}2]$ axis (details are shown in the supplementary material). In the coarse-grained domain away from the GB, 3D rhombohedral elements are designed to expose the {111} slip planes in face-centered cubic (FCC) Ni. Each element in the coarse-grained domain is embedded with 2197 atoms, whose displacements were interpolated from finite element nodal displacement through a first-order shape function. The grain that contains the dislocation pile-up (Grain 1) extends 1 μm along the slip direction to accommodate 15 built-in full mixed dislocations with Burgers vector $\vec{\boldsymbol{b}} = \boldsymbol{a/2\langle 110\rangle}$, which disassociate into leading and trailing partials. Such a coarse-grained domain is shown to be sufficiently large to preserve the long-range stresses induced by the dislocation pileup. Shear stresses are applied at a strain rate of 2×10^7/s to drive these dislocations to migrate along the (111) slip plane and interact with the atomically structured GB.

Figure 5a presents two snapshots from the simulation of the interaction between a pile-up of dislocations and the GB (one is prior to transmission and the other is after transmission) colored by the magnitude of RSS. A Virial stress formula as discussed in [27] was used to calculate the local stresses at the atomic level. The evolution of the atomistic structure at the slip-GB intersection can be directly extracted from the model and is included in the inset in Fig. 5a. It shows that the GB reconfigures before and after the transmission. This GB structure reconfiguration is accompanied by an increase in dislocation density near the GB and a change of the local stress state. To track the local stress evolution, at each time step, the simulation cell is divided into a number of bins (each bin has a width of ~3nm) along *y* direction. The stress in each bin is calculated from the average of the local stresses. A plot of the stress as a function of the position of the bin leads to the stress profile along *y* direction (pile-up direction). Figure 5b shows the four

representative stress profiles when the sample is under four different shear strains (noted as ε). The top view of the reaction process at different ε are shown in Figure 5c-f, in which only the positions of those defected atoms are displayed and color coded (blue indicates stacking faults, red for leading and trailing end of dislocations and GB) by Common Neighbor Analysis using OVITO [28]. Three observations from Figure 5b are: (i) at ε = 2.8% (orange curve), there is a high local stress concentration at a level of ~3.4 GPa ahead of the pileup due to the accumulation of dislocations at the GB. It should be noted that, because of the significantly higher resolution (bin size of ~3nm) for the local stress calculation in CAC than that in experiments, the magnitude of the stress concentration from simulations is significantly higher than the experimental results shown in Figures 2-4. Nevertheless, both experiments and CAC simulations confirm that there is a significant internal stress build up when a large number of dislocation-mediated slip are blocked by the GB. (ii) As the shear strain increased from ε = 2.8% to 3.04% (red and yellow curves in Fig. 5b), a dislocation loop embryo starts to nucleate (Fig. 5d-e), however it did not cause an immediate drop in the stress concentration. This is qualitatively consistent with the experimental observation that the stress drop does not correlate directly with the formation of a slip band in the neighboring grain. (iii) At ε = 3.28% (purple curve in Fig. 5b), a significant stress reduction from ~3.4 GPa to ~2.4 GPa at the pileup tip is observed. This reduction is found to be caused by the dislocation loop migration away from the GB (see Fig. 5e-f). Upon a further strain increase in our CAC simulations, we observe many cycles of stress build-up and reduction. The magnitude of stress reduction is found to be at a level of ~0.5 GPa, compared to ~1.0 GPa, in the first drop as seen in Fig. 5b. This suggests that the pileup-induced peak stress at the pileup tip may saturate if many dislocations transfer across the GBs at the same site.

In summary, through *in situ* HR-EBSD experimental analysis of the slip-GB interactions in plastically deformed polycrystalline Ni, we provide direct evidence of: (a) the high local internal stress buildup induced by the formation of dislocation pileups during slip-GB interactions; (b) the persistency of such high local stresses even after the outgoing slip system activates at the GB; (c) stress relaxation when more dislocations arrive and push out the newly nucleated dislocations at the slip-GB intersection; (d) the saturation of nucleation-/transmission-induced stress concentrations. These experimental observations are supplemented and explained by the results from a high-fidelity CAC simulation. An integration of CAC with HR-EBSD study of the slip-GB reactions can potentially be used for obtaining slip transfer related parameters, such as the magnitude of saturation stress for different GBs, the evolution of the stress tensor, and even how the GB structure is reconfigured after slip transfer. This information can be helpful for formulating new metrics that can incorporate the local stress complexity for understanding the process of slip transfer across GBs and can provide needed inputs for microstructure-sensitive finite element analysis.

Acknowledgements

YS and JK acknowledge support from the U.S. National Science Foundation (DMR -2043264). TP and LX acknowledge the support of the U.S. National Science Foundation (CMMI-1930093) and the Extreme Science & Engineering Discovery Environment (XSEDE-TG-MSS170003, 190008, and 190013).

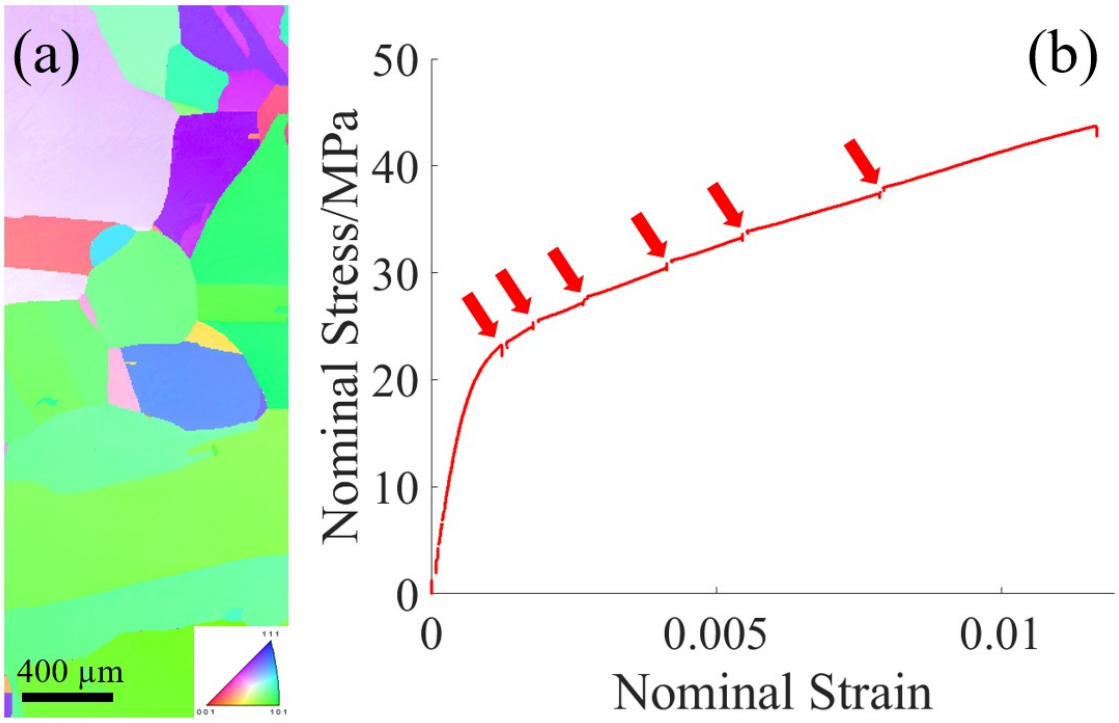

Figure 1: (a) Inverse pole figure map of the sample studied. (b) Nominal stress/strain curve of the *in situ* uniaxial tension test. The discontinuities in the curve indicate the strain levels at which the test was paused for HR-EBSD analysis.

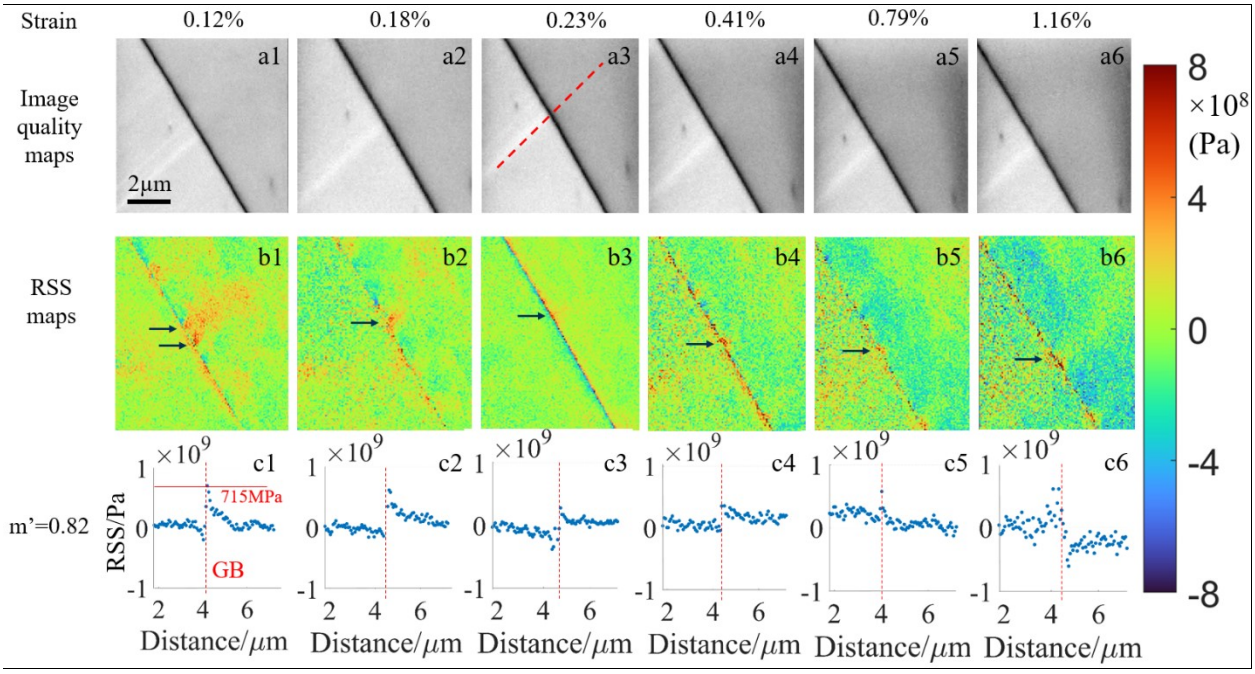

Figure 2: (a1-a6) Image quality maps showing a slip band interacting with a GB with m'=0.82, the incoming slip bands start from the lower left corner and stopps at the grain boundary. (b1-b6) RSS maps showing the magnitude of RSS at each grid point. Areas with high and low value of RSS are colored by red and blue, respectively, while the areas with negligible RSS are colored in green. Locations of the slip band/GB interactions are indicated by black arrows. It is worth noting that in b1 there are slip systems interacting with the GB, while as the strain increases only one (lower) system remains active. (c1-c6) RSS values plotted along the incoming slip band (red dotted line in a3 for example). Locations of the GBs are indicated by a vertical red line.

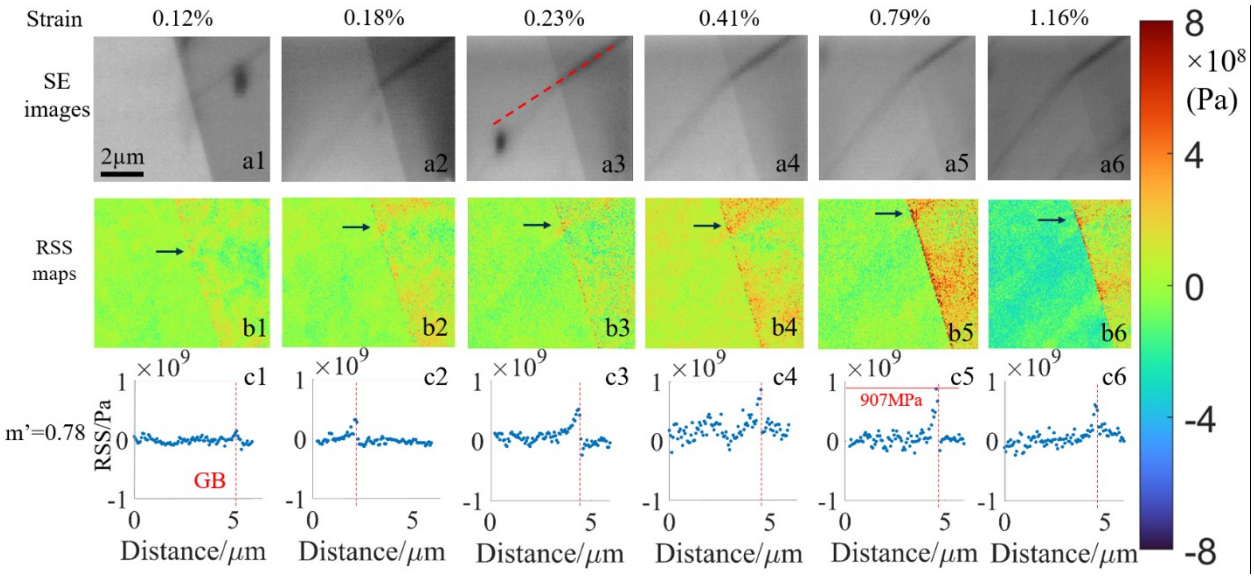

Figure 3: (a1-a6) Secondary electron images showing a slip band interacting with a GB with m'=0.78, the incoming slip bands start from the upper right corner and stop at the grain boundary. (b1-b6) RSS maps showing the magnitude of RSS at each grid point. (c1-c6) RSS values plotted along the incoming slip band (red dotted line in a3 for example).

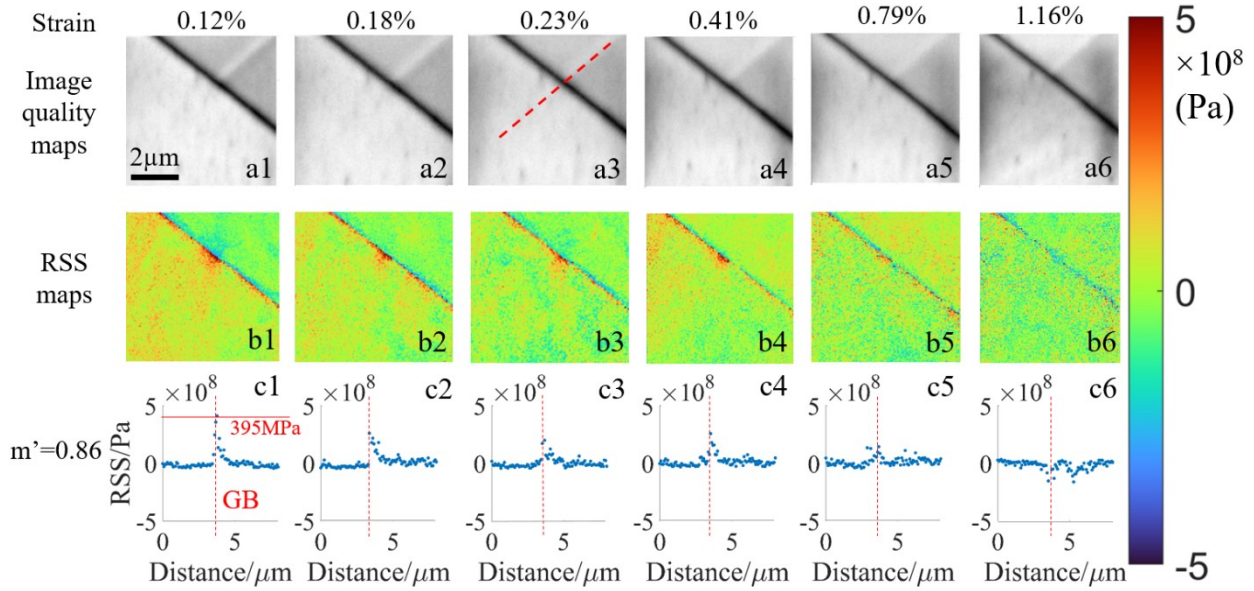

Figure 4: (a1-a6) Image quality maps showing a slip band interacting with a GB with m'=0.86, the incoming slip bands start from the upper right corner and stop at the grain boundary. (b1-b6) RSS maps showing the magnitude of RSS at each data point. (c1-c6) RSS values plotted along the incoming slip band (red dotted line in a3 for example).

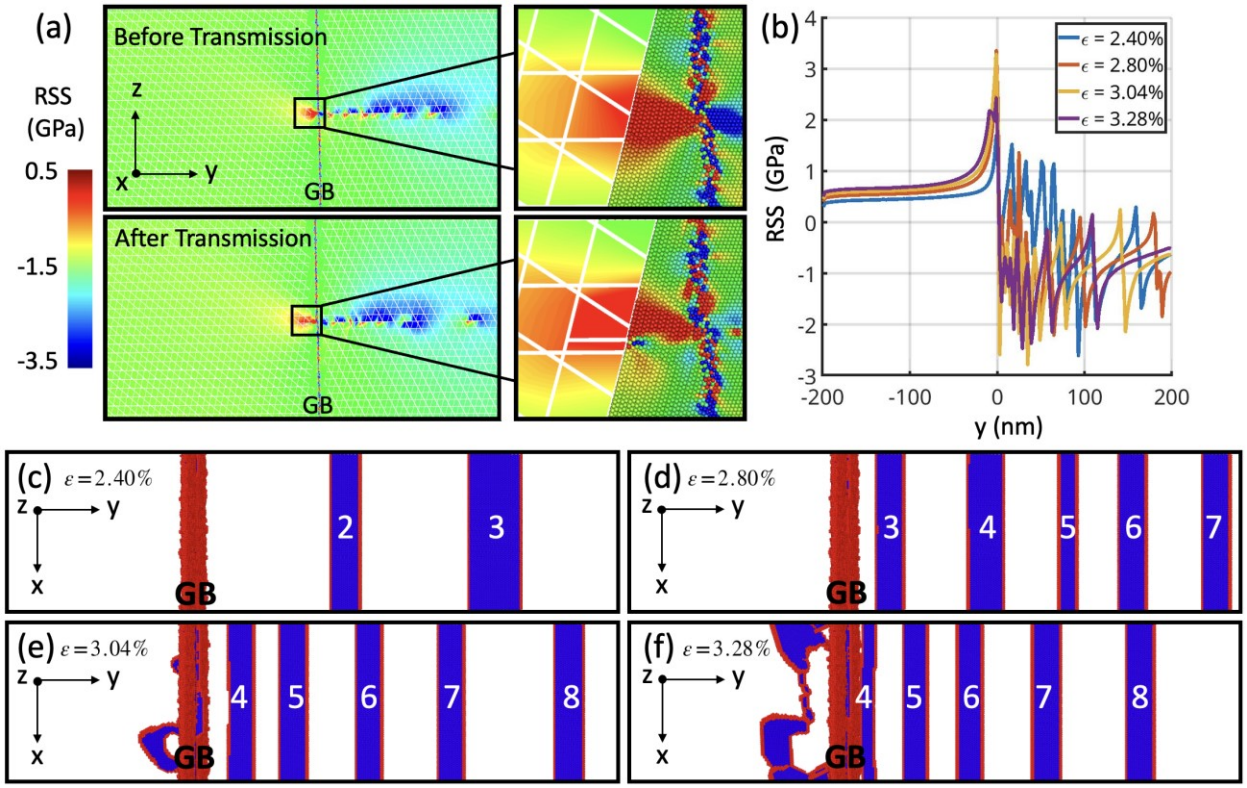

Figure 5: (a) The shear stress contour together with the atomistic structure evolution at the GB during a dislocation slip-GB interaction (before and after the first dislocation transmission); (b) Evolution of the stress profiles along the dislocation slip direction across the GB at various applied strain levels; (c-f) Top views of the process of the interaction between a queue of incoming dislocations from the right and an atomically structured GB at different strain levels corresponding to each curve in (b). Numbers are the indices of dislocations initially built in, lower index means closer to the GB initially. Atoms are color coded by Common Neighbor Analysis (blue are of hexagonal close-packed structure indicating stacking faults and red are not of any crystal structure indicating leading and trailing ends of dislocations and the GB). All atoms of FCC structure are deleted to only display dislocations, stacking faults, and the GB.

References:

[1] J. Kacher, B.P. Eftink, B. Cui, I.M. Robertson, Dislocation interactions with grain boundaries, Curr. Opin. Solid State Mater. Sci. 18 (2014) 227-243.

[2] L. Wang, Y. Yang, P. Eisenlohr, T.R. Bieler, M.A. Crimp, D.E. Mason, Twin nucleation by slip transfer across grain boundaries in commercial purity titanium, Metall. Mater. Trans. A 41 (2010) 421-430.

[3] B.A. Simkin, B.C. Ng, M.A. Crimp, T.R. Bieler, Crack opening due to deformation twin shear at grain boundaries in near-γ TiAl, Intermetallics. 15 (2007) 55-60.

[4] Z. Shen, R.H. Wagoner, W.A.T. Clark, Dislocation and grain boundary interactions in metals, Acta Metall. 36 (1988) 3231-3242.

[5] J. Luster, M.A. Morris, Compatibility of deformation in two-phase Ti-Al alloys: Dependence on microstructure and orientation relationships, Metall. Mater. Trans. A 26 (1995) 1745-1756.

[6] T.C. Lee, I.M. Robertson, H.K. Birnbaum, An *In Situ* transmission electron microscope deformation study of the slip transfer mechanisms in metals, Metall. Mater. Trans. A 21 (1990) 2437-2447.

[7] J. Kacher, I.M. Robertson, In situ and tomographic analysis of dislocation/grain boundary interactions in α-titanium, Phil. Mag. 94 (2014) 814-829.

[8] Y. Su, S. Han, P. Eisenlohr, M.A. Crimp, Predicting shear transmission across grain boundaries with an iterative stress relief model, Acta Mater. 215 (2021) 116992.

[9] T.R. Bieler, R. Alizadeh, M. Peña-Ortega, J. Llorca, An analysis of (the lack of) slip transfer between near-cube oriented grains in pure Al, Int. J. Plast. 118 (2019) 269-290.

[10] Y. Su, C. Zambaldi, D. Mercier, P. Eisenlohr, T.R. Bieler, M.A. Crimp, Quantifying deformation processes near grain boundaries in α titanium using nanoindentation and crystal plasticity modeling, Int. J. Plast. 86 (2016) 170-186.

[11] Y. Guo, T.B. Britton, A.J. Wilkinson, Slip band–grain boundary interactions in commercial-purity titanium, Acta Mater. 76 (2014) 1-12.

[12] R. Sperry, A. Harte, J.Q. Fonseca, E.R. Homer, R.H. Wagoner, D.T. Fullwood, Slip band characteristics in the presence of grain boundaries in nickel-based superalloy, Acta Mater. 193 (2020) 229-238.

[13] E. Nieto-Valeiras, J. Llorca, Criteria for slip transfer across grain and twin boundaries in pure Ni, Materialia. 21 (2022) 101303.

[14] A.J. Wilkinson, G. Meaden, D.J. Dingley, High-resolution elastic strain measurement from electron backscatter diffraction patterns: new levels of sensitivity, Ultramicroscopy 106 (2006) 307-313.

[15] J. Kacher, C. Landon, B.L. Adams, D. Fullwood, Bragg's Law diffraction simulations for electron backscatter diffraction analysis, Ultramicroscopy 109 (2009) 1148-1156.

[16] A. Koko, E. Elmukashfi, T.H. Becker, P.S. Karamched, A.J. Wilkinson, T.J. Marrow, In situ characterisation of the strain fields of intragranular slip bands in ferrite by high-resolution electron backscatter diffraction, Acta Mater. 239 (2022) 118284.

[17] D.E. Spearot, M.D. Sangid, Insights on slip transmission at grain boundaries from atomistic simulations, Curr. Opin. Solid State Mater. Sci. 18 (2014) 188-195.

[18] B. Liu, D. Raabe, P. Eisenlohr, F. Roters, A. Arsenlis, G. Hommes, Dislocation interactions and low-angle grain boundary strengthening, Acta Mater. 59 (2011) 7125-7134.

[19] S. Xu, L. Xiong, Y. Chen, D.L. McDowell, Sequential slip transfer of mixed-character dislocations across Σ3 coherent twin boundary in FCC metals: a concurrent atomistic-continuum study, Npj Comput. Mater. 2 (2016) 15016.

[20] T. Ma, H. Kim, N. Mathew, D.J. Luscher, L. Cao, A. Hunter, Dislocation transmission across Σ3{112} incoherent twin boundary: a combined atomistic and phase-field study, Acta Mater. 223 (2022) 117447.

[21] H. Lim, M. Lee, J. Kim, B. Adams, R. Wagoner, Simulation of polycrystal deformation with grain and grain boundary effects, Int. J. Plast. 27 (2011) 1328-1354.

[22] Y. Peng, R. Ji, T. Phan, W. Gao, V.I. Levitas, L. Xiong, An atomistic-to-microscale computational analysis of the dislocation pileup-induced local stresses near an interface in plastically deformed two-phase materials, Acta Mater. 226 (2022) 117663.

[23] OpenXY, https://github.com/BYU-MicrostructureOfMaterials/OpenXY.

[24] B. Kuhr, D. Farkas, Dislocation content in random high angle grain boundaries, Modelling Simul. Mater. Sci. Eng. 27 (2019) 045005

[25] L. Xiong, G. Tucker, D.L. McDowell, Y. Chen, Coarse-grained atomistic simulation of dislocations, J. Mech. Phys. Solids, 59 (2) (2011) 160-177.

[26] L. Xiong, Y. Chen, Coarse-grained simulations of single-crystal silicon, Model. Simul. Mater. Sci. Eng., 17 (3) (2009) 035002.

[27] J. Rigelesaiyin., A. Diaz, W. Li, L. Xiong, Y. Chen, Asymmetry of the atomic-level stress tensor in homogeneous and inhomogeneous materials, Proc. R. Soc. A 474 (2018) 20180155.

[28] A. Stukowski, Visualization and analysis of atomistic simulation data with OVITO–the Open Visualization Tool, Model. Simul. Mater. Sci. Eng. 18 (2010) 015012.

Supplementary material (details of the CAC model set up):

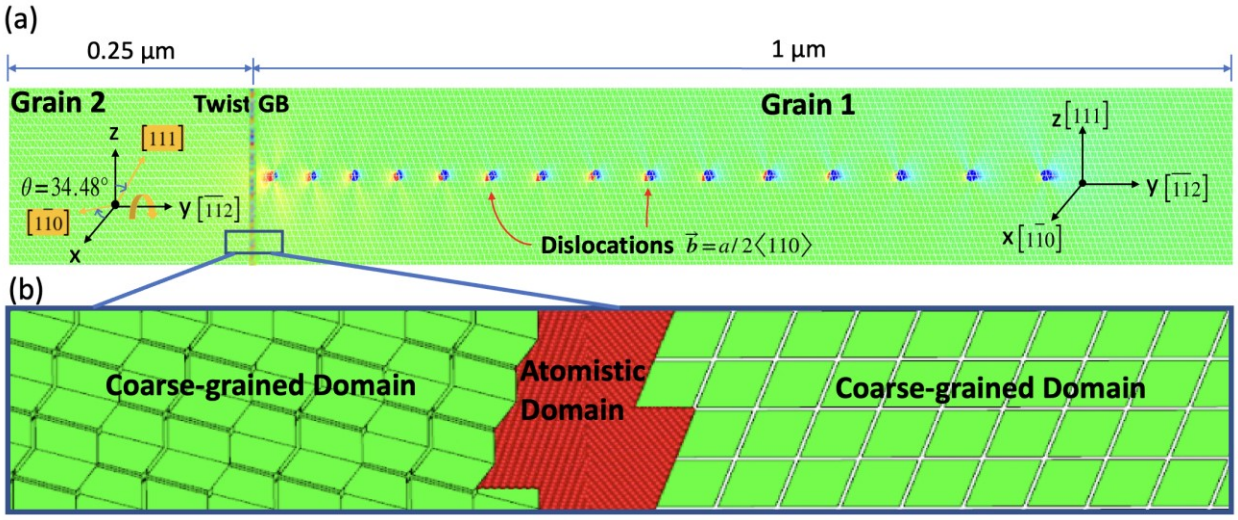

Supplementary figure 1: The CAC model set-up of bi-crystal FCC Ni to closely resemble the GB in Figure 2 with m' = 0.82: (a) dislocations are built into Grain 1 and pile up at the twist GB interface; (b) a zoom-in view of a region around the GB showing the atomistic resolution near the GB and coarse-grained description far away.